

INFORMED WATERMARK EMBEDDING IN THE FRACTIONAL FOURIER DOMAIN

Oktay Altun, Gaurav Sharma, Mark Bocko

Department of Electrical and Computer Engineering
University of Rochester
Rochester, NY, 14627-0126

ABSTRACT

We propose an informed watermark embedding method in fractional Fourier domain. Detectability and imperceptibility of the watermark sequence constraints as well as real-valuedness in spatial domain are imposed on the resulting image using a set theoretic framework. Insertion of multiple bits without using a block based scheme is also a novel approach and provides improvement against synchronization attacks. The watermarked image is determined using the method of projections onto convex sets (POCS) to simultaneously satisfy the multiple constraints. A performance comparison between blind and informed embedding is illustrated and experimental results are presented to show the effectiveness of the informed method.

1. INTRODUCTION

Watermarking with blind detection can be modelled as communication with side information. This effort has two main branches: Informed coding and informed embedding [1]. In informed coding the codeword representing watermark signal is generated depending on the original cover file. However in informed embedding, which will be our main concern in this paper, already coded watermark signal is shaped depending on the cover signal.

Watermark embedding is usually performed by adding a watermark pattern to the cover data without distorting the fidelity of the cover data. The cover data is treated as noise and this kind of embedding is known as “blind embedding”. However, it has already been illustrated in the literature that the watermark embedder can be more effective since the cover data is known to the embedder during watermark insertion. This embedding strategy is referred as “informed embedding” [2].

The fractional Fourier domain is a time-frequency representation of the signal. Embedding watermark sequences into fractional Fourier domain has an important advantage over embedding spatial domain or frequency domain. Watermark in fractional Fourier domain provides extra security against attackers since angle(s) of the transform provides extra degree of freedom [3]. Recent work in cryptanalysis of watermarks has proven to be effective in estimating and removing the watermark sequences. Mihcak et al estimate 90% of the DSSS sequence by MAP estimation [4]. However, embedding into fractional domains will make these endeavors ineffective due to the extra degree of freedom given by fractional Fourier angles.

This nice feature of embedding into fractional Fourier domain has attracted attention and a blind embedding technique is proposed by Djurovic et al [3]. However, it is not an easy task to extend their algorithm to informed watermarking because the visual models are defined either in time domain or frequency domain. Defining these models again in fractional domains is a tedious and unnecessary task.

Here we propose an informed embedding method in the fractional Fourier domain. The method implicitly shapes the watermark power to the signal content by imposing constraints that ensures imperceptibility, detectability, real-valuedness and robustness to compression. The watermarked image is determined to satisfy these constraints using a POCS algorithm [5]. Insertion of multiple bits without using a block structure provides extra easiness against de-synchronization attacks since synchronizing one pn-sequence gives synchronization with the rest of the watermark pn-sequences.

We recently introduced a set-theoretic framework for watermarking and a POCS based technique [5]. In this paper, we specifically address time-frequency domains, which offer some significant differences and advantages.

2. FRACTIONAL FOURIER TRANSFORM

The one dimensional fractional Fourier transform of a signal $x(t)$ is defined as:

$$X(u) = \int_{-\infty}^{+\infty} x(t) \cdot K(u, t) \cdot dt \quad (1)$$

where $K(u, t)$ is a transform kernel, given by:

$$K(u, t) = \sqrt{\frac{1 - j \cdot \cot(\alpha)}{2}} \cdot e^{j \cdot (t^2 + u^2) \cot \alpha / 2 - j u t \csc \alpha} \quad (2)$$

Two dimensional fractional Fourier transform can be obtained by successively taking one dimensional fractional Fourier transforms of rows and columns due to the separability of the transform. The signal obtained is in purely time domain if transformation angle is 0 and in purely frequency domain if angle is $\pi/2$. A fast algorithm has been developed for fractional Fourier transform which is also an attractive feature for watermark embedding purposes. [6].

3. FRACTIONAL FOURIER DOMAIN WATERMARKING USING POCS

In POCS method two important assumptions are made: Each a priori information or desired property restricts the solution to a convex set in Hilbert space H and the desired signal lie

This work was supported by the Air Force Research Laboratory/IFEC under grant number F30602-02-1-0129.

in the intersection of all of these sets which represent the space of acceptable solutions. The sequence of successive projections onto these sets weakly converges to a point on the boundary of intersection of all of these sets.

POCS can be used as a method to embed watermarks into multimedia by defining suitable constraint sets that insure imperceptibility and detectibility of the embedded watermark [5]. Fractional Fourier domain watermarking can be accomplished using the sets described in the following section.

The convexity of the constraints is easy to see and will not be proved here. The projection operations are written as a constrained optimization problem and solved by Lagrange multiplier method. Successive projections are done by order and weakly converges to the intersection of the sets:

$$f_{k+1} = (P_{S_n}(P_{S_{n-1}} \dots P_{S_1}(f_k) \dots)), \quad k = 0, 1, \dots \quad (3)$$

The projections are performed by using Lagrange multipliers. Details of the projections can be found in [5].

$$X_{i+1} = P_j(X_i) = \arg \min_{X \in S_j} \|X - X_i\| \quad (4)$$

4. CONVEX CONSTRAINTS FOR FRACTIONAL FOURIER DOMAIN WATERMARKING

In order to obtain a watermarked signal using POCS we define the following constraints:

4.1 Real-valuedness:

Modifying the signal in fractional Fourier domain for the purpose of embedding will most probably disrupt the real-valuedness of the signal in time domain. In our method we define the constraint of real-valuedness :

$$S_1 \equiv \{X \in \mathbb{C}^{NXN} : X - \text{Re}(X) = 0\} \quad (5)$$

In [3], the problem is solved by adding the same watermark signal into fractional Fourier domain with transform angle $-\alpha$. However, this approach may introduce extra distortion to keep the signal real.

4.2 Detectibility:

The second constraint below in equation 6 ensures the detectibility of the watermark by the receiver. Contrary to the additive approach, successive projections will eliminate the interference due to the host signal. The dot product is defined on vectors and not matrices, so we first arranged X and W to a row or column vector to form X^* and W^* . The permutation operation performed is not important if same permutation is used for both X^* and W^* . We assumed the detector side does not have the original image hence decodes the watermark blindly.

$$S_2 \equiv \{X \in \mathbb{R}^{NXN} : \frac{1}{N \times M} W^{*T} \text{FrFT}(X^*) \geq \} \quad (6)$$

It is worth mentioning that, an operationally equivalent formulation of this detection scheme can be obtained by

preprocessing¹ the watermark sequence and embedding into spatial domain instead of embedding into fractional Fourier domain, due to the linearity and separability of Fractional Fourier transform. Both of the schemes can be used for extra degree of freedom due to estimation attacks. An equivalent formulation is as follows:

$$S'_2 \equiv \{X \in \mathbb{R}^{NXN} : \frac{1}{N \times M} \text{FrFT}(W^{*T})X^* \geq \} \quad (7)$$

4.3 Pointwise Fidelity:

The visual fidelity of the image is guaranteed by two visual constraints. The first one is imposed by a spatial domain texture masking model. Pereira et al. has proposed this visual model which outputs allowable distortion at pixel level given the original image. [7] The constraint below in equation 8 illustrates the resulting convex set where where X is an image size matrix which lies in the allowable lower (L) and upper (U) bounds.

$$S_3 \equiv \{X \in \mathbb{R}^{NXN} : L \leq X \leq U\} \quad (8)$$

4.4 Overall Fidelity:

The second visual model is proposed by Mannos et al [8]. They have proposed a visual distortion metric for monochrome images which takes into account of the fact that human observer is more sensitive to some spatial frequencies than others and he is more sensitive to intensity errors in gray regions than white. He formulates a parametric filter based on experimental results which we use in our method. The second constraint is formulated as an inequality that forces the overall visual distortion metric of the image be smaller than some threshold value. $\|\cdot\|$ represents Euclidean distance, $H(w)$ is the filter in frequency domain and X_0 represents the original image.

$$S_4 \equiv \{X \in \mathbb{C}^{NXN} : \|H(w) \cdot X(w) - H(w) \cdot X_0(w)\| < \} \quad (9)$$

4.5 Robustness To Compression

The requirement of robustness to compression can be roughly expressed by the following mathematical expression:

$$S_5 \equiv \{X \in \mathbb{R}^{NXM} : \frac{1}{N \times M} W^* \cdot \text{IDCT}(Q[\text{DCT}(X^*)]) \geq \} \quad (10)$$

where Q stands for JPEG quantization scheme, DCT and IDCT represents discrete cosine transform and inverse discrete cosine transform respectively. However, this constraint is not convex.

So we approximated it with the following equation:

$$\hat{S}_5 \equiv \{X \in \mathbb{R}^{NXM} : \frac{1}{N \times M} W^* \cdot \text{IDCT}(Q_{NZ(X_0)}[\text{DCT}(X^*)]) \geq \} \quad (11)$$

¹We would like to thank one of the anonymous reviewers for bringing this to our attention.

where $Q_{NZ}(x_0)$ refers to the non-zero quantized DCT coefficients of the original image. This approximation has the underlying assumption that the DCT coefficients that is quantized to zero after compression is causing the major loss of watermark information.

5. RESULTS AND ANALYSIS

We have designed an experiment to compare the performance of blind embedding with respect to informed embedding. To obtain an estimate of the capacity of the blind embedding, we started to embed bits to achieve a certain detection rate. We continue on embedding extra bits until the invisibility of the watermark is disrupted. Then we measure the total number of embedded bits and report the capacity as the blind watermark capacity.

We could insert only 5 bits into fractional Fourier domain without distorting the visual texture noise masking model. Although exceeding a single pixel interval may not be noticed in the whole image, the result of the experiment illustrates the success of the POCS method in embedding 100 bits without violating any visual constraint. The bit error rate in both of the embedding was zero, we could detect all the bits without error.

		S_0	S_1	Q_R
1	$2.5 \cdot 10^6$	30	3	60

Table 1: Particularities of the models for POCS based algorithm.

We inserted 100 bits into Goldhill image's real part of the $_1 = 0.7 \cdot \sqrt{2}$ and $_2 = 0.7 \cdot \sqrt{2}$ fractional Fourier transform by successive projections onto convex sets that we have defined previously. One can also choose values randomly for each bit using a cryptographic key for security purposes. We decided to stop inserting bits when the POCS algorithm started to converge slowly and the new projections started to erase the previous information we have inserted. The detector response of the correlated watermark sequence and uncorrelated random sequence is illustrated in figure 4.

To illustrate the success of the method in cancelling the source interference cancellation, we embedded 100 bits by blind embedding method. The histogram of the detector response is shown in 3. Bit error rate is 86% when we set the detection threshold to 0.75.

Figure 1 and Figure 2 illustrates the performance of visual fidelity of both methods. In figure 1 the watermark noise is disturbing especially in flat regions of the image. POCS is very successful in shaping the watermark noise and distributing the power in more busy regions.

To get rid of the complexity due to two visual fidelity criteria in our analysis, we assume that the overall visual dis-

	Capacity	Bit Error Rate
Blind	5 bits	0
Informed	100 bits	0

Table 2: Experimental capacity of both blind and informed embedding. 512x512 pseudo-random sequence is used for each bit.



Figure 1: A portion of blindly watermarked Goldhill image. PSNR of the whole image is 31 dB. 100 bits inserted. BER=8%.



Figure 2: A portion of Goldhill image watermarked by POCS. PSNR of the whole image is 30 dB. 100 bits inserted. BER=0%.

tortion metric constraint is not binding. The upper allowable pixel level (U) and lower allowable pixel level (L) are the only factors that limits channel capacity. Furthermore, we assume the texture noise masking model is very accurate and signal in this interval is totally imperceptible. Any signal distortion beyond this interval makes the watermark perceptible and it is not a valid watermark embedding.

In this scenario, the payload capacity of the watermark is primarily limited by the smallest interval in the allowable variations determined by the visual texture noise masking model. We obtained the payload capacity values with an intuitive approach. The payload capacity for the cover image is mainly restricted by the upper and lower limits in spatial domain. For blind case, minimum interval determines the bottleneck of the capacity. $\frac{2}{W}$ represents watermark variance (power) for each pixel. The signal power in fractional domain will be preserved in time domain due to the Parseval's theorem for fractional Fourier transforms, so the watermark variance $\frac{2}{W}$ can be used interchangeably in calculations. So, for the blind case watermark payload capacity can be approx-

imated as follows:

$$C_p \approx \frac{\text{Total energy available for watermark}}{\text{Average Watermark Power For Each Bit}} \quad (12)$$

$$C_p \approx \frac{[\min_i(U_i - L_i)]^2}{\frac{2}{W}} \quad (13)$$

In POCS embedding, the resulting signal beyond L and U are tailored by projection onto the visual texture constraint and watermark power is distributed to rest of the intervals to achieve the predetermined detector response rate. So, the overall upper and lower bounds can be treated as one channel for the whole watermark with energy $\frac{2}{W} \cdot N^2$.

$$C'_p \approx \frac{[\sum_i (U_i - L_i)^2]}{\frac{2}{W} \cdot N^2} \quad (14)$$

We have embedded watermark without using any blocking structure. All bits are inserted to the same space-frequency slice. This property is worth mentioning due to its advantages for de-synchronization attacks. For detector side, the endeavor for re-synchronization all bits is as simple as re-synchronization one bit since every bit shares the same time-frequency window. Robustness to compression constraint increases the robustness of the watermark against compression and is discussed in depth in [5].

The algorithm converges in 30 iterations. It takes less than 10 minutes to embed 100 bit watermark with a Pentium M 1.8 GHz processor computer.

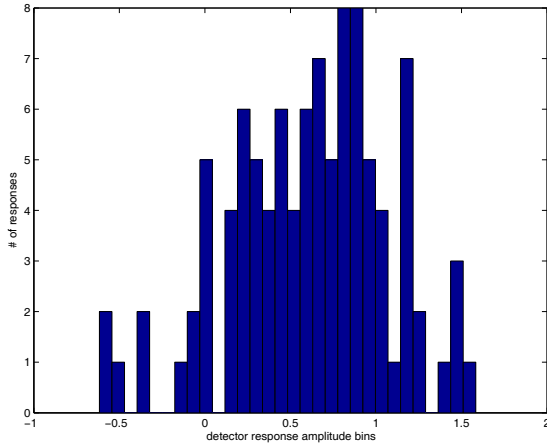


Figure 3: Histogram of detector response for blindly watermarked image. 100 bits inserted, watermark size is equal to image size.

6. CONCLUSION

In this paper we have introduced a set theoretic fractional Fourier domain watermark embedding technique for monochrome images. The proposed technique can be readily applied to any watermarking technique currently using spread spectrum and can easily be adopted for color images as well. We have shown that POCS is a very efficient method for informed watermark embedding and can improve the watermark insertion capacity into fractional Fourier domains sig-

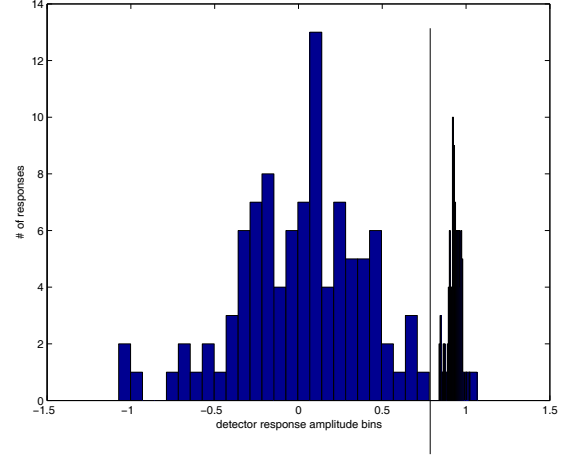


Figure 4: Histogram of detector response for informed watermarking. Left hand side of the threshold line illustrates detector response of uncorrelated sequence. Right hand side of the threshold line illustrates detector response of watermark sequence. 100 bits inserted, watermark size is equal to image size.

nificantly without distorting visual fidelity. The multi-bit watermark embedding without blocking property is especially beneficial for dealing with de-synchronization attacks.

REFERENCES

- [1] M. L. Miller, G. J. Doerr, and I. J. Cox, "Applying informed coding and embedding to design a robust, high capacity watermark," *IEEE Trans. on Image Processing*, vol. 13, no. 6, pp. 792–807, Jun. 2004.
- [2] I. J. Cox, M. L. Miller, and J. A. Bloom, "Digital watermarking," *Morgan Kaufmann*, 2001.
- [3] Igor Djurovic, Srdjan Stankovic, and Ioannis Pitas, "Digital watermarking in the fractional fourier transformation domain," *Journal of Network and Computer Applications*, vol. 24, no. 4, pp. 167–173, Jul. 2001.
- [4] M. K. Mihcak, R. Venkatesan, and M. Kesal, "Cryptanalysis of discrete-sequence spread spectrum watermarks," in *Proceedings of the 5th International Information Hiding Workshop (IH 2002)*, Noordwijkerhout, The Netherlands, Oct. 2002.
- [5] O. Altun, G. Sharma, M. Celik, and M. Bocko, "Semifragile hierarchical watermarking in a set theoretic framework," in *Submitted and Accepted to be presented, ICIP*, 2005.
- [6] H. M. Ozaktas, Z. Zalevsky, and M. Kutay, "The fractional fourier transform," in *John Wiley and Sons*, 2001.
- [7] T. Pun S. Pereira, S. Voloshynskiy, "Optimal transform domain watermark embedding via linear programming," *Signal Processing*, vol. 81, no. 6, pp. 1251–1260, Jun. 2001.
- [8] J. L. Mannos and D. L. Sakrison, "The effects of a visual fidelity criterion on the encoding of images," *IEEE Transactions on Information Theory*, vol. 20, no. 4, pp. 525–536, Jul. 1974.